

## ORIGINAL ARTICLE

# Identification and validation of a poor clinical outcome subtype of primary prostate cancer with Midkine abundance

Quan Zhou<sup>1,2</sup> | Chen Yang<sup>1,2,3</sup> | Zezhong Mou<sup>1,2</sup> | Siqi Wu<sup>1,2</sup> | Xiyu Dai<sup>1,2</sup> |  
Xinan Chen<sup>1,2</sup> | Yuxi Ou<sup>1,2</sup> | Limin Zhang<sup>1,2</sup> | Jianjun Sha<sup>4</sup> | Haowen Jiang<sup>1,2,3</sup> 

<sup>1</sup>Department of Urology, Huashan Hospital, Fudan University, Shanghai, China

<sup>2</sup>Fudan Institute of Urology, Huashan Hospital, Fudan University, Shanghai, China

<sup>3</sup>National Clinical Research Center for Aging and Medicine, Fudan University, Shanghai, China

<sup>4</sup>Department of Urology, Renji Hospital, School of Medicine, Shanghai Jiao Tong University, Shanghai, China

## Correspondence

Limin Zhang and Haowen Jiang, Department of Urology, Huashan Hospital, Fudan University, Shanghai 200040, China.

Emails: [zhalim@fudan.edu.cn](mailto:zhalim@fudan.edu.cn); [haowj\\_sh@fudan.edu.cn](mailto:haowj_sh@fudan.edu.cn)

Jianjun Sha, Department of Urology, Ren Ji Hospital, School of Medicine, Shanghai Jiao Tong University, Shanghai 200001, China.

Email: [shajianjunrj@126.com](mailto:shajianjunrj@126.com)

## Funding information

National Natural Science Foundation of China, Grant/Award Number: 81872102

## Abstract

Recent studies identified Midkine (MDK) as playing a key role in immune regulation. In this study, we aimed to discover the clinical significance and translational relevance in prostate cancer (PCa). We retrospectively analyzed 759 PCa patients who underwent radical prostatectomy from Huashan Hospital, Fudan University (training cohort,  $n = 369$ ) and Chinese Prostate Cancer Consortium (validation cohort,  $n = 390$ ). A total of 325 PCa patients from The Cancer Genome Atlas (TCGA) database (external cohort) were analyzed for exploration. Immune landscape and antitumor immunity were assessed through immunohistochemistry and flow cytometry. Patient-derived explant culture system was applied for evaluating the targeting potential of MDK. We found that intratumoral MDK expression correlated with PCa progression, which indicated an unfavorable biochemical recurrence (BCR)-free survival for postoperative PCa patients. Addition of MDK expression to the postoperative risk assessment tool CAPRA-S could improve its prognostic value. Tumors with MDK abundance characterized the tumor-infiltrating CD8<sup>+</sup> T cells with less cytotoxicity production and increased immune checkpoint expression, which were accompanied by enriched immunosuppressive contexture. Moreover, MDK inhibition could reactivate CD8<sup>+</sup> T cell antitumor immunity. MDK mRNA expression negatively correlated with androgen receptor activity signature and positively associated with radiotherapy-related signature. In conclusion, intratumoral MDK expression could serve as an independent prognosticator for BCR in postoperative PCa patients. MDK expression impaired the antitumor function of CD8<sup>+</sup> T cells through orchestrating an immunoevasive microenvironment, which could be reversed by MDK inhibition. Moreover, tumors with MDK enrichment possessed potential sensitivity to postoperative radiotherapy while resistance to adjuvant hormonal therapy of PCa. MDK could be considered as a potential therapeutic target for PCa.

**Abbreviations:** AR, androgen receptor; BCR, biochemical recurrence; GSEA, gene set enrichment analysis; IF, immunofluorescence; IHC, immunohistochemical; MDK, Midkine; PBMC, peripheral blood mononuclear cell; PCa, prostate cancer; PDE, patient-derived explant; PRAD, prostate adenocarcinoma; PSA, prostate-specific antigen; RP, radical prostatectomy; TCGA, The Cancer Genome Atlas; TMA, tumor microarray.

Quan Zhou, Chen Yang, Zezhong Mou, and Siqi Wu contributed equally to this work.

This is an open access article under the terms of the [Creative Commons Attribution-NonCommercial](https://creativecommons.org/licenses/by-nc/4.0/) License, which permits use, distribution and reproduction in any medium, provided the original work is properly cited and is not used for commercial purposes.

© 2022 The Authors. *Cancer Science* published by John Wiley & Sons Australia, Ltd on behalf of Japanese Cancer Association.

## KEYWORDS

adjuvant therapy, biochemical recurrence, CD8<sup>+</sup> T cell, Midkine, prostate cancer

## 1 | INTRODUCTION

Prostate cancer (PCa) is the most prevalent cancer worldwide, which caused around 300,000 global mortalities in 2020.<sup>1</sup> Radical prostatectomy (RP) surgery is still employed as one of the main therapeutic approaches for localized PCa.<sup>2</sup> Biochemical recurrence (BCR) occurs in several patients after RP, accompanied by a high risk for mortalities and metastasis.<sup>3</sup> Systematic predictors of BCR based on existing clinicopathological features are well adopted in clinical practice.<sup>4,5</sup> However, predictors show a relatively low precision for evaluating BCR events for PCa patients.<sup>6</sup> Molecular biomarkers for predicting BCR and improving the accuracy of existing systematic predictors are in urgent need.<sup>7</sup>

Meanwhile, a variety of therapies have emerged through these decades including hormonal therapy and radiotherapy for postoperative or advanced PCa.<sup>8-10</sup> Advanced genomic signatures and molecular classifications have been discovered for personalized therapies,<sup>11,12</sup> and predictive biomarkers for guiding individualized therapies are being pursued.<sup>7</sup>

Midkine (MDK) is a heparin-binding growth factor which plays vital roles in malignant pathogenesis.<sup>13</sup> Recent studies have explored that MDK serves as a modulator that orchestrates an immunosuppressive microenvironment in aggressive melanoma.<sup>14</sup> Moreover, MDK expressed by NF1-mutant brain neurons activates naïve CD8<sup>+</sup> T cells to produce Ccl4 resulting in robust tumor progression in gliomas.<sup>15</sup> However, whether MDK orchestrates immune suppression in PCa remains ambiguous. Emerging studies have focused on the role of immune contexture, especially CD8<sup>+</sup> T cells in PCa progression.<sup>16-18</sup> Hence, in this study we explored the clinical significance and translational relevance of MDK in PCa.

Our results demonstrated that MDK abundance characterized an inferior prognosis subset of postoperative PCa patients with dampened intratumoral CD8<sup>+</sup> T cell cytotoxicity. Intratumoral MDK expression showed close association with resistance to adjuvant hormonal therapy and sensitivity to postoperative radiotherapy. Moreover, MDK could act as a potential therapeutic target for PCa.

## 2 | METHODS

### 2.1 | Study population

Seven hundred and fifty-nine PCa patients who underwent RP were enrolled and eventually selected from two clinical centers: Huashan Hospital of Fudan University from 2007 to 2020 ( $n = 369$ , named training cohort) and Chinese Prostate Cancer Consortium from 2013 to 2018 ( $n = 390$ , named validation cohort). The enrollment flowchart is displayed in (Figure 1A). The inclusion criteria were as

follows: (a) informed consent; (b) performed RP; (c) without neoadjuvant therapy; (d) available for formalin-fixed and paraffin-embedded tumor tissues. Respectively, 20 and 30 patients from the training and validation cohorts were excluded for the following exclusion criteria: (a) lack of clinical data or incomplete follow-up information; (b) diagnosed as nonprostate adenocarcinoma; (c) tissue detachment from tumor microarrays (TMAs). High-risk PCa was defined as tumor with prostate-specific antigen (PSA) > 20 ng/ml and/or Gleason score > 7 and/or pT > 2 and/or pN1. The postoperative follow-up data were updated in January 2021. Tissues from both cohorts were formalin fixed and paraffin embedded, which were then prepared as TMAs.

Tumor characteristics of 333 patients with prostate adenocarcinoma of The Cancer Genome Atlas (TCGA-PRAD) were obtained from a previous study,<sup>12</sup> which were then named external cohort. The clinical and follow-up data were obtained from <http://www.cbioportal.org> at Feb. 2020. Eight samples were excluded due to the lack of follow-up information. Finally, 325 patients with available clinical information and mRNA data were included for analysis.

Twenty-two fresh tumor samples from Huashan Hospital were collected after RP for flow cytometry analysis. Fourteen fresh tumor samples from Huashan Hospital were obtained for ex vivo culture experiment termed patient-derived explant (PDE) culture system.

### 2.2 | Assay methods

Immunohistochemical (IHC) staining was performed on TMA slides as described previously.<sup>19</sup> Each entire set of TMA slides was subjected to IHC staining at the same time for an objective evaluation for all samples. Immunofluorescence (IF) staining was performed for M1 (CD68<sup>+</sup> CD206<sup>+</sup>) and M2 macrophages (CD68<sup>+</sup> CD206<sup>-</sup>) staining, of which CD68 (ab955, Abcam) and CD206 (ab64693, Abcam) antibodies were utilized. Briefly, after dewaxing and antigen retrieval, TMA slides were incubated with primary antibodies in a wet chamber at 4 C overnight. The secondary antibodies which were conjugated to FITC or cyanine three dyes were then applied for TMA slides with tyramide signal amplification system (PerkinElmer). VECTASHIELD with DAPI (Vector Laboratories) was utilized for nucleus staining and prolonging the storage. Slides were scanned by TissueFAXS Plus (TissueGnostics).

The IHC score of MDK (ab52637, Abcam) was evaluated and calculated based on the staining intensity and staining proportion by two pathologists who were blinded to the clinical characteristics. Briefly, the staining intensity was stratified as zero (negative), one (weak), two (moderate), and three (strong). The staining proportion of positive staining area was scored from 0% to 100%. IHC

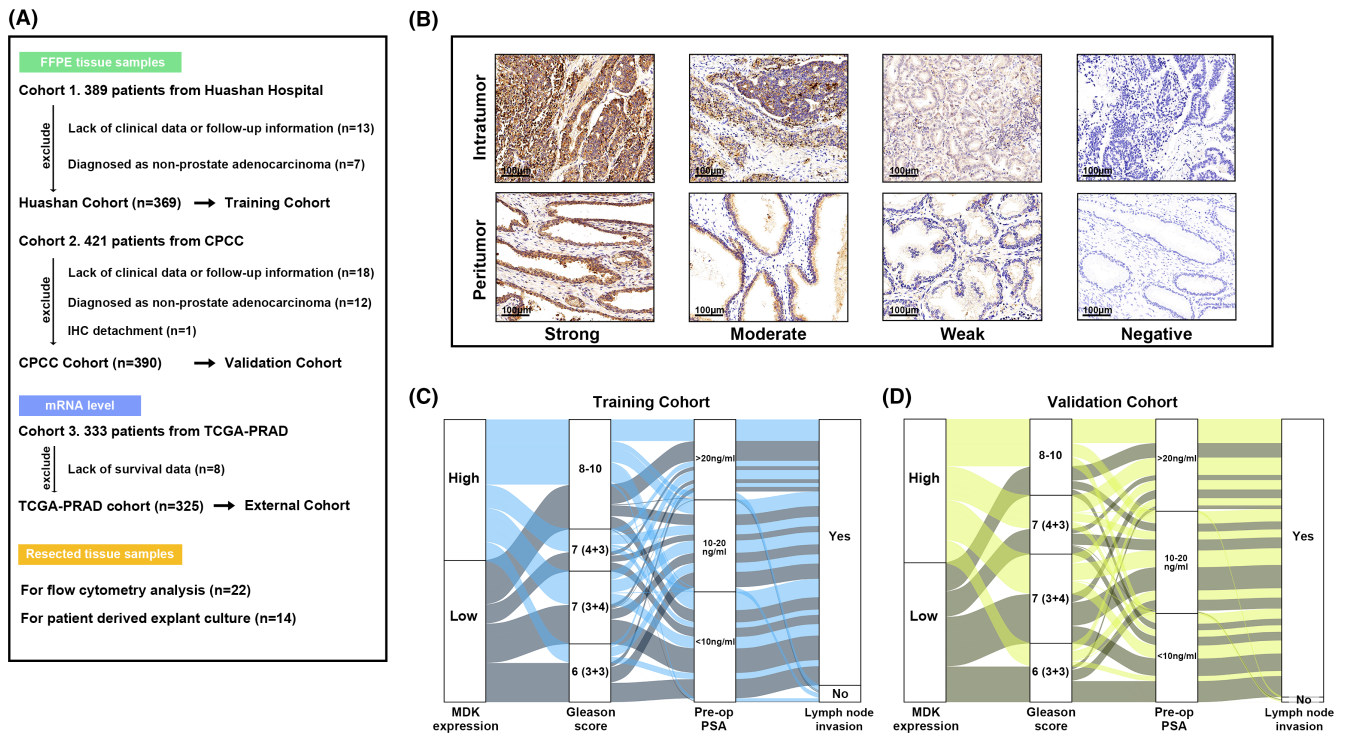


**FIGURE 1** Midkine expression during tumor progression in PCa patients. (A) The flowchart demonstrating the patients enrolled in training, validation and external cohort. (B) Representative IHC staining images illustrating intratumoral and peritumoral MDK expression based on negative, weak, moderate and strong staining intensity. (C and D) The Sankey diagrams illustrating the association of intratumoral MDK expression with Gleason score, preoperative PSA levels and lymph node invasion.

score ranging from 0 to 300 was finally calculated by multiplying the staining intensity and staining proportion. Tumor-infiltrating CD8<sup>+</sup> T cells (ab17147, Abcam), CD4<sup>+</sup> T cells (ab67001, Abcam), mast cells (ab2378, Abcam), M1 macrophages, M2 macrophages were quantified as the mean value of three randomized high-power magnification fields (x200 magnification) of tumor regions in each sample. The expression of PD-L1 (ab228462, Abcam) and HLA class I (ab225636, Abcam) were semiquantified according to previous studies on PCa.<sup>20,21</sup> Briefly, PD-L1 expression was scored based on the staining intensity as negative, weak, moderate, and strong. The score of HLA class I staining was categorized as 0, 1, or 2, defined as membrane staining in 0%-20%, 20%-80%, and 80%-100% of tumor cells, respectively. The cutoff values for intratumoral and peritumoral MDK expression were the median values of respective IHC scores in the training cohort, which were then applied for the validation cohort for consistency. The cutoff value for tumor-infiltrating CD8<sup>+</sup> T cells was the median value of infiltration quantification.

### 2.3 | Flow cytometry methods

Fresh tumor samples were obtained immediately after surgical resection, of which adipose or necrotic tissues were removed carefully. To collect single-cell suspensions, tumors were minced and digested in RPMI-1640 with collagenase I (Sangon; 250 U ml<sup>-1</sup>) and DNase I (Sangon; 50 U ml<sup>-1</sup>) for 3 hours at 37°C according to the instructions.

Red blood cell lysis buffer was then used for removing red blood cells. After stimulation with cell stimulation cocktail (PMA and ionomycin, eBioscience) and Golgistop (BD Biosciences) for 4 hours, cells were stained with membrane markers in dark for 45 minutes at 4°C after applying Human Fc block (BD Biosciences). Cells were stained with intracellular markers after permeabilization by the BD Cytofix/Cytoperm Fixation/Permeabilization Solution Kit (BD Biosciences) or BD Pharmingen Transcription Factor Buffer Sets (BD Biosciences). Detailed information on antibodies for flow cytometry is listed in Table S1. Cells were collected and analyzed on the FACSCelesta (BD Biosciences) in 1 hour. In addition, part of the fresh tumor tissues was formalin fixed and paraffin embedded for MDK IHC staining to stratify the tumor into high/low intratumoral MDK expression groups.

### 2.4 | In vitro assays for T cell analysis

Peripheral blood mononuclear cells (PBMCs) were isolated from 5 PCa patients by applying Ficoll-Paque Plus (GE Healthcare) through density gradient centrifugation. CD8<sup>+</sup> T cells were isolated and collected from PBMCs by using a CD8<sup>+</sup> T Cell Isolation Kit (Miltenyi Biotec) according to the manufacturer's instructions. The expression of LRP1 and LRP6 on the PBMC-isolated CD8<sup>+</sup> T cells was detected through flow cytometry. Meanwhile, CD8<sup>+</sup> T cells were activated by Cloudz Human T Cell Activation Kit (R&D Systems) and recombinant IL-2 (Abcam) in RPMI-1640 medium with 10% fetal bovine

serum and 1% penicillin-streptomycin solution plus the treatment with 10ng/ml recombinant MDK (MDKr, Beyotime) and 20ug/ml anti-LRP1 (ThermoFisher) for 48 hours. CD8<sup>+</sup> T cells were then collected and underwent flow cytometry analysis.

## 2.5 | Ex vivo culture system

The ex vivo culture system termed PDE was constructed as previously well described.<sup>22,23</sup> Previous studies have confirmed that the PDE model could maintain the native tumor microenvironment and tumor tissue viability.<sup>24,25</sup> Briefly, the presoaked gelatin sponge was placed in 24-well plates containing 500  $\mu$ l media (RPMI-1640 with 10% fetal bovine serum, 1% penicillin-streptomycin solution, 0.01 mg/ml hydrocortisone, and 0.01 mg/ml insulin) and appropriate treatment (10ng/ml MDKr [Beyotime] or 1  $\mu$ M MDK inhibitor [MDKi, Sigma]). Fresh PCa samples were immediately obtained after RP and subdivided into 1 mm<sup>3</sup> pieces. One or two pieces were placed on each sponge, and 24-well plates were then placed in an incubator for 24 hours at 37°C and 5% CO<sub>2</sub>. Tissues were finally digested into single-cell suspensions and underwent flow cytometry analysis.

## 2.6 | Statical methods

Biochemical recurrence was defined as two continuous PSA  $\geq$ 0.2 ng/ml after RP. BCR-free survival time was calculated from the date of RP till the date of BCR or last follow-up. Patients who were alive or BCR-free were censored.

Kaplan-Meier curves and univariate/multivariate Cox regression analyses were applied for analyzing survival outcomes. The progenitor-exhausted and terminally exhausted CD8<sup>+</sup> T cell signatures were obtained from a previous study.<sup>26</sup> The androgen receptor (AR) output score, AR activity signature, and postoperative radiation therapy score were obtained from previous studies.<sup>8,10,12</sup> The gene signatures utilized in this study are listed in Table S2. Gene set enrichment analysis (GSEA) was conducted for exploring the potential activated pathways. Chi-square test, one-way ANOVA with Bonferroni correction, Kruskal-Wallis H test, Wilcoxon matched-pairs signed-rank test, Mann-Whitney U test, and Spearman's correlation test were performed for analysis. *P* values were considered statistically significant when  $<0.05$ .

# 3 | RESULTS

## 3.1 | Patient and tumor characteristics of the study population

The flowchart of the study is illustrated in (Figure 1A). The patient and tumor characteristics of the training cohort and validation cohort are demonstrated in Table 1. Clinical features of both

cohorts were in agreement with the acknowledged demographics of PCa with RP. The 5-year BCR-free survival rates in validation, training, and external cohorts were 70.2%, 81.1%, and 75.6% respectively.

## 3.2 | Midkine expression correlated with tumor progression in PCa

Midkine expression in PCa was assessed by IHC staining. The representative images of intratumoral and peritumoral MDK expression with strong, moderate, weak, and negative staining are displayed in (Figure 1B). The median H-score values of intratumoral and peritumoral MDK expression were both 120 in the training cohort, which were then applied as the cutoff values in the validation cohort. Moreover, in the training and validation cohorts, we found that intratumoral MDK expression correlated with the increasing Gleason score (chi-square test:  $p = 0.007$  and  $p = 0.015$ ) and preoperative PSA level (chi-square test:  $p = 0.006$  and  $p < 0.001$ ), indicating a strong relationship between MDK and PCa tumor progression (Figure 1C,D). In addition, the MDK mRNA expression was elevated with the increasing Gleason score in the external cohort (Figure S1A). Our findings indicated a close correlation between MDK and tumor progression.

## 3.3 | Intratumoral MDK expression was a strong prognosticator for clinical outcome of PCa

The prognostic value of MDK for postoperative PCa was next evaluated. Kaplan-Meier analysis showed that high intratumoral MDK expression could predict an unfavorable BCR-free survival in both the training cohort ( $p < 0.001$ ; Figure 2A) and validation cohort ( $p = 0.001$ ; Figure 2B). Five-year BCR-free survival rates were 59.5% versus 84.9% and 72.6% versus 89.8% for high versus low intratumoral MDK expression in both cohorts, respectively. Additionally, high MDK mRNA expression in the external cohort indicated poor prognosis of PCa patients ( $p = 0.024$ ; Figure S1B). However, peritumoral MDK expression failed to stratify the BCR-free survival in both cohorts (Figure 2C,D). Univariate Cox regression analysis demonstrated that high intratumoral MDK expression was associated with shortened BCR-free survival (Table S3). Moreover, through the multivariate Cox regression analysis for MDK expression and other clinicopathological features, intratumoral MDK expression was identified as an independent prognosticator for BCR in both the training cohort and validation cohort (Figure 2E).

Subgroup analysis was conducted, and it was found that intratumoral MDK expression correlated with poor prognosis in the subgroup with Gleason score  $<7$  or  $\geq 7$  (Figure S2A–D) and in the low- and intermediate-risk or high-risk group (Figure S3A–D). Therefore, we assumed that intratumoral MDK expression could act as an outstanding prognosticator for postoperative PCa.

Characteristics	Training cohort (n = 369)	Validation cohort (n = 390)	Pooled patients (n = 759)
Age, years			
Median	68	70	70
Range	47-84	47-87	47-87
Prostatectomy grade groups			
GG1	76 (20.6%)	81 (20.8%)	157 (20.7%)
GG2	95 (25.7%)	123 (31.5%)	218 (28.7%)
GG3	55 (14.9%)	81 (20.8%)	136 (17.9%)
GG4	49 (13.3%)	70 (17.9%)	119 (15.7%)
GG5	94 (25.5%)	35 (9.0%)	129 (17.0%)
Pre-op PSA			
<10	144 (39.0%)	122 (31.3%)	266 (35.0%)
10-20	120 (32.5%)	141 (36.2%)	261 (34.4%)
>20	105 (28.5%)	127 (32.6%)	232 (30.6%)
Lymph node involvement			
Absent	347 (94.0%)	383 (98.2%)	730 (96.2%)
Present	22 (6.0%)	7 (1.8%)	29 (3.8%)
Neural invasion			
Absent	257 (69.6%)	221 (56.7%)	478 (63.0%)
Present	112 (30.4%)	169 (43.3%)	281 (37.0%)
Positive surgical margin			
Absent	319 (86.4%)	381 (97.7%)	700 (92.2%)
Present	50 (13.6%)	9 (2.3%)	59 (7.8%)
Extracapsular extension			
Absent	346 (93.8%)	332 (85.1%)	678 (89.3%)
Present	23 (6.2%)	58 (14.9%)	81 (10.7%)
Seminal vesicle invasion			
Absent	307 (83.2%)	375 (96.2%)	682 (89.9%)
Present	62 (16.8%)	15 (3.8%)	77 (10.1%)
Events			
Biochemical recurrence	71 (19.2%)	80 (20.5%)	151 (19.9%)

**TABLE 1** Baseline demographics and clinical characteristics of PCa patients

Abbreviations: GG, grade group; PCa, prostate cancer; Pre-op PSA, preoperative prostate-specific antigen.

### 3.4 | Intratumoral MDK expression improved the risk stratification by CAPRA-S score

The CAPRA-S score is a postsurgical score previously established for predicting the PCa recurrence based on the surgical-related pathological characteristics.<sup>4</sup> We tried to evaluate whether the intratumoral expression of MDK could add prognostic value to the CAPRA-S score system. The CAPRA-S score baseline of the training and validation cohorts are listed in Table S4. Univariate Cox regression analysis confirmed that the CAPRA-S score was a strong prognosticator in both the training and validation cohorts (Table 2). With the C-index analysis, we found that the CAPRA-S score plus the intratumoral MDK expression had a higher C-index than the CAPRA-S score alone, inferring that intratumoral MDK expression could help improve the risk stratification by the CAPRA-S score (Table 2).

### 3.5 | CD8<sup>+</sup> T cells showed impaired antitumor immunity in PCa with MDK expression abundance

Recent studies have revealed the potential immune-modulating capacity of MDK leading to tumor progression.<sup>13,15</sup> Kaplan-Meier analysis was performed for comparing the BCR-free survival with CD8<sup>+</sup> T cell infiltration and intratumoral MDK expression strata. Contrary to most tumor types, CD8<sup>+</sup> T cell infiltration was associated with poor prognosis in PCa ( $p = 0.036$ ; Figure 3A and Figure S4A). It was found that high CD8<sup>+</sup> T cell infiltration indicated a worse BCR-free survival in the high MDK expression group, while there was no association between CD8<sup>+</sup> T cell infiltration and BCR-free survival in the low MDK expression group (Figure 3B). However, a similar infiltration level of CD8<sup>+</sup> T cells was observed in tumors with high/low intratumoral MDK expression (Figure S4B). Also, the proportion of CD8<sup>+</sup> T cells

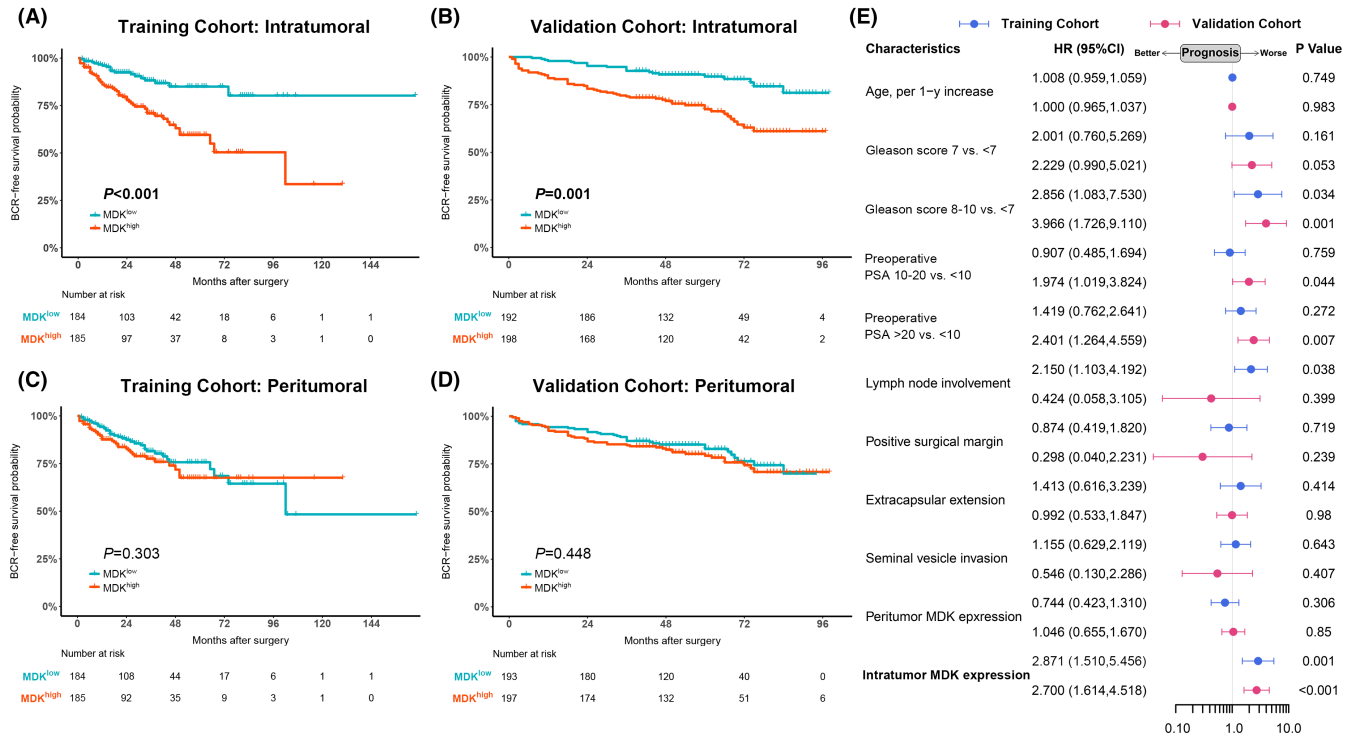


**FIGURE 2** Intratumoral MDK expression yields poor prognosis of postoperative PCa patients. (A and B) Kaplan-Meier curves for BCR-free survival comparing tumor with high versus low intratumoral MDK expression in training cohort (A) and validation cohort (B). (C and D) Kaplan-Meier curves for BCR-free survival comparing tumor with high versus low MDK peritumoral expression in training cohort (C) and validation cohort (D). (E) Multivariate cox regression analysis of BCR-free survival for intratumoral and peritumoral MDK expression with clinicopathological characteristics. Solid horizontal lines in red and blue represented variables in training cohort and validation cohort respectively. Log-rank *p* values were shown.

**TABLE 2** Multi- and univariate Cox regression analyses of CAPRA-S with/without intratumoral MDK expression for BCR-free survival

Variable	Model with intratumoral MDK expression				Model without intratumoral MDK expression			
	Training Cohort		Validation Cohort		Training Cohort		Validation Cohort	
	HR (95% CI)	P	HR (95% CI)	P	HR (95% CI)	P	HR (95% CI)	P
CAPRA-S	1.164 (1.063-1.275)	0.001	1.166 (1.051-1.293)	0.004	1.209 (1.108-1.319)	<0.001	1.222 (1.107-1.350)	<0.001
Intratumoral MDK expression (high versus low)	2.514 (1.467-4.307)	0.001	2.466 (1.490-4.083)	<0.001	/	/	/	/
C-index of the model <sup>a</sup>	0.754 (0.703-0.806)	/	0.699 (0.637-0.762)	/	0.652 (0.595-0.708)	/	0.649 (0.583-0.714)	/

Abbreviations: BCR, biochemical recurrence; CI, confidence interval; HR, hazard ratio; MDK, Midkine.

<sup>a</sup>The C-index was provided for continuous CAPRA-S with/without dichotomized intratumoral MDK expression (high versus low).

among CD45<sup>+</sup> cells between tumors with high versus low MDK expression showed no difference (Figure S4C). We suggested that MDK expression could interfere with the antitumor activity of CD8<sup>+</sup> T cells rather than act as a chemoattractant in PCa. It was further discovered that MDK mRNA expression showed no association with the progenitor-exhausted signature (Figure 3C), while it was positively correlated with the terminally exhausted signature (Figure 3D) in the external cohort. The phenotype of tumor-infiltrating CD8<sup>+</sup> T cells

was next evaluated in fresh tumor tissues via flow cytometry. Gating strategy and representative flow cytometry images were illustrated in Figure S5A,B. It was found that CD8<sup>+</sup> T cells expressed decreasing cytolytic capacity (GZMB and PRF1) and downregulated the effector molecule (IFN-γ) in tumors with MDK abundance (Figure 3E-J). Furthermore, the expression of PD-1 and Tim-3 was upregulated on CD8<sup>+</sup> T cells in tumors with high intratumoral MDK expression (Figure 3K-M). The proportion of CD8<sup>+</sup> T cells with the expression

of certain molecules in CD45<sup>+</sup> cells was next evaluated. Decreased infiltration of CD8<sup>+</sup> T cells with GZMB, PRF1, and IFN- $\gamma$  expression while increased infiltration of CD8<sup>+</sup> T cells with PD-1 and Tim-3 expression were found in tumors with MDK abundance (Figure 3N). Thus, we inferred that intratumoral MDK expression was associated with the dysfunction state of CD8<sup>+</sup> T cell in PCa.

### 3.6 | Midkine shows direct but faint immunosuppressive effect on CD8<sup>+</sup> T cells

Whether MDK could directly or indirectly influence the function of CD8<sup>+</sup> T cells was further explored. A previous study reports that T cells express a moderate level of Lrp1 and a low level of Lrp6, which are both the receptors of MDK. We found that PBMC-isolated CD8<sup>+</sup> T cells partly expressed LRP1 (16.80% $\pm$ 7.91%), while LRP6 was rarely detected (1.18% $\pm$ 0.92%; Figure S6A). The PBMC-isolated CD8<sup>+</sup> T cells were incubated with MDKr and anti-LRP1 neutralizing antibody. It was found that the administration of MDKr elevated the PD-1 expression of CD8<sup>+</sup> T cells and only decreased the production of GZMB, while other antitumor molecules remained on the same production level (Figure S6B–D), which was inconsistent with the findings in Figure 3K–M. Moreover, the effect of MDKr treatment on CD8<sup>+</sup> T cells could be reversed by anti-LRP1 treatment (Figure S6B–D). We suggested that MDK had a direct but faint immunosuppressive effect on CD8<sup>+</sup> T cells.

### 3.7 | Elevated expression of PD-L1 and infiltration of M2 macrophages are observed in PCa with MDK enrichment

As MDK showed a direct but weak effect on CD8<sup>+</sup> T cells, we postulated that tumors with MDK abundance might be enriched with immunosuppressive components resulting in tumor progression. A high proportion of strong and moderate PD-L1 staining in PCa with high MDK expression was observed (Figure S7A,B). However, no difference of HLA class I was observed in PCa with high versus low intratumoral MDK expression (Figure S7C,D).

As for the immune contexture in PCa, we found that neither the infiltration of CD4<sup>+</sup> T cells nor the CD4/CD8 ratio showed any difference between tumors with high versus low intratumoral MDK expression (Figure S8A–C). Although no different infiltration of M1 macrophages was observed in tumors with high versus low intratumoral MDK expression (Figure S8D,E), it was found that tumors with MDK abundance were infiltrated with increasing M2 macrophages (Figure S8F). The M1/M2 ratio was decreased in tumors with high MDK expression (Figure S8G), inferring that M2 macrophage polarization occurred. Moreover, protumor mast cells were enriched with high intratumoral MDK expression in PCa (Figure S8H–I).<sup>27</sup> Therefore, we suggested that MDK expression orchestrated an immunosuppressive microenvironment in PCa leading to CD8<sup>+</sup> T cell dysfunction.

### 3.8 | Intratumoral MDK expression could serve as a potential therapeutic target for PCa

The PDE culture system was utilized to examine the effect of MDK on CD8<sup>+</sup> T cell function and PCa cell apoptosis (Figure 4A). It was discovered that treatment with MDKr impaired the expression of GZMB and PRF1 of tumor-infiltrating CD8<sup>+</sup> T cells (Figure 4B) in tumors with low intratumoral MDK expression, and the IFN- $\gamma$  production showed a decrease with marginal significance (Figure 4C). MDKr treatment also promoted the PD-1 and Tim-3 expression of CD8<sup>+</sup> T cells (Figure 4D). Meanwhile, the administration of MDKi successfully enhanced the antitumor immunity of CD8<sup>+</sup> T cells featuring increased production of GZMB, PRF1, and IFN- $\gamma$  and decreased expression of PD-1 and Tim-3 in tumors with high intratumoral MDK expression (Figure 4B–D). Moreover, elevated annexin V expression of tumor cells was detected with the intervention of MDK (Figure 4E). With the help of the PDE culture system, we suggested that MDK may be considered as a potential therapeutic target for PCa.

### 3.9 | Intratumoral MDK expression correlates with distinct molecular subtypes in PCa patients

We finally explored the association of MDK with previously reported molecular subtypes.<sup>12</sup> It was found that tumor with MDK abundance was enriched in mRNA cluster 2 and miRNA cluster 2,5 and 6 (Figure 5A,B). Moreover, a higher level of copy number alteration of TP53, PTEN, and FANCC was observed in tumors with high MDK expression than in those with low MDK mRNA expression (Figure 5C–E). Several genomic signatures associated with postoperative PCa were previously discovered, which could potentially support the choice of adjuvant therapies including hormonal therapy and radiotherapy (Figure S9A–C).<sup>8,10,12</sup> GSEA showed a downregulation of AR response in tumors with high MDK expression (Figure 5F). The AR activity signature and AR output score negatively correlated with MDK expression (Figure 5G,H).<sup>8,12</sup> We suggested that tumors with MDK abundance may be characterized by hormonal therapeutic resistance. Moreover, a 24-gene predictor for the postoperative radiotherapy was positively associated with MDK expression in PCa,<sup>10</sup> indicating that tumors with high MDK expression were potentially sensitive to postoperative radiotherapy (Figure 5I). These results demonstrated MDK expression might act as a biomarker for guiding the postoperative adjuvant therapy for PCa patients.

## 4 | DISCUSSION

In this study, we focused on the clinical significance and therapeutic relevance of MDK expression in PCa. MDK has been found to have a key role in tumorigenesis and has been identified as a prognostic biomarker in other cancer types including pancreatic cancer, bladder cancer, and hepatocellular carcinoma.<sup>13,28–30</sup> It was discovered for the first time that MDK expression could act as a prognosticator

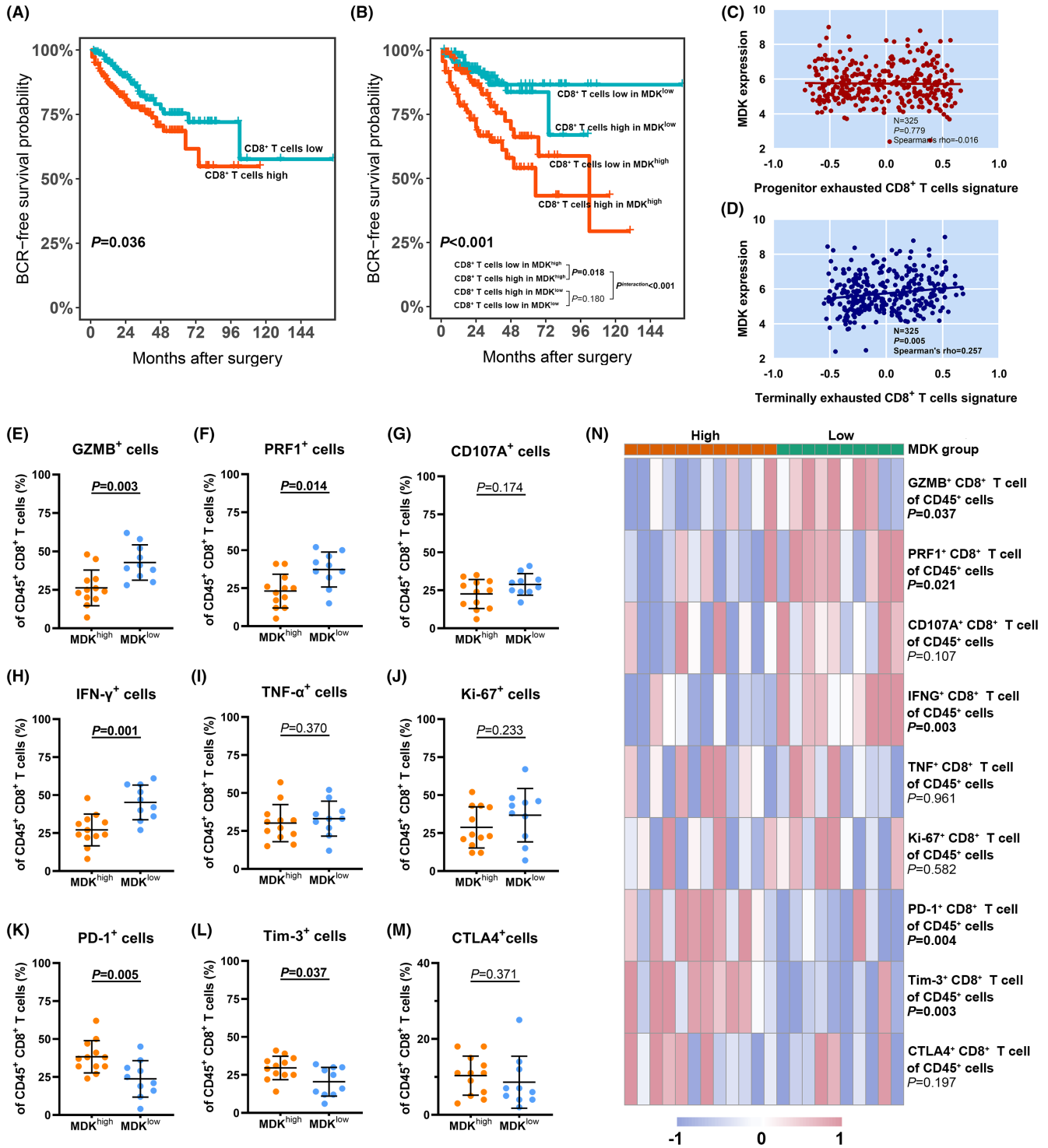


**FIGURE 3** Tumor-infiltrating CD8<sup>+</sup> T cell features an exhausted phenotype with dampened cytotoxicity in tumors with intratumoral MDK abundance. (A) Kaplan-Meier curves for BCR-free survival with tumor-infiltrating CD8<sup>+</sup> T cells strata in training cohort (n = 369). (B) Kaplan-Meier curves for BCR-free survival with both tumor-infiltrating CD8<sup>+</sup> T cells and intratumoral MDK expression strata in training cohort (n = 369). Log-rank p values were shown. (C and D) Correlation between MDK mRNA expression and progenitor exhausted (C) or terminally exhausted (D) CD8<sup>+</sup> T cells signature. Data was analyzed by Spearman correlation. (E-G) Evaluation of cytotoxicity expression (GZMB, PRF1 and CD107A) of tumor-infiltrating CD8<sup>+</sup> T cells in high/low intratumoral MDK expression groups. (H-J) Evaluation of effector expression (IFN-γ and TNF-α) and proliferative marker (Ki-67) of tumor-infiltrating CD8<sup>+</sup> T cells in high/low intratumoral MDK expression groups. (K-M) Evaluation of immune checkpoint (PD-1, Tim-3 and CTLA4) expression of tumor-infiltrating CD8<sup>+</sup> T cells in high/low intratumoral MDK expression groups. (N) Heatmap illustrating the proportion of CD8<sup>+</sup> T cells expressing abovementioned cytotoxicity, effector, proliferative and immune checkpoint molecules in CD45<sup>+</sup> cells in tumors with high (n = 12) or low (n = 10) intratumoral MDK expression. Data were analyzed with Mann-Whitney U test.

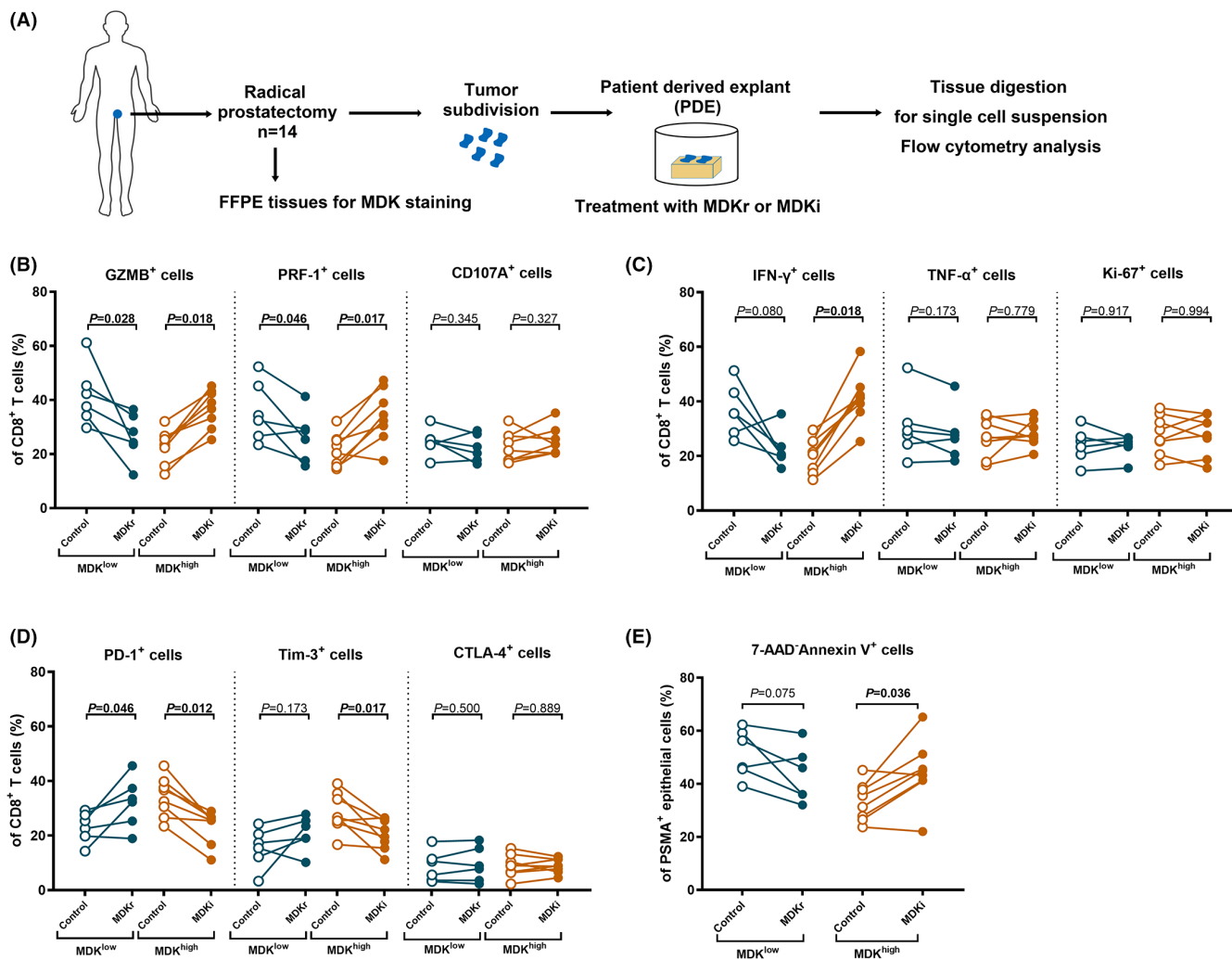


**FIGURE 4** Intratumoral MDK expression could serve as a potential therapeutic target for PCa. (A) The schematic of PDE model construction was illustrated. (B) Evaluation of cytotoxicity expression (GZMB, PRF1 and CD107A) of CD8<sup>+</sup> T cells in PDE models treated with MDKr or MDKi based on the intratumoral MDK expression in control group. (C) Evaluation of effector expression (IFN- $\gamma$  and TNF- $\alpha$ ) and proliferative marker (Ki-67) of CD8<sup>+</sup> T cells in PDE models treated with MDKr or MDKi based on the intratumoral MDK expression in control group. (D) Evaluation of immune checkpoint (PD-1, Tim-3 and CTLA4) of CD8<sup>+</sup> T cells in PDE experiments treated with MDKr or MDKi based on the intratumoral MDK expression in control group. (E) Evaluation of Annexin V expression of PSMA<sup>+</sup> epithelial cells in PDE experiments treated with MDKr or MDKi based on the intratumoral MDK expression in control group. Data were analyzed with Wilcoxon matched-pairs signed-rank test.

for BCR in postoperative PCa patients. The risk assessment tool CAPRA-S was utilized to predict the postoperative clinical outcome based on clinicopathological characterizations.<sup>4</sup> Intratumoral MDK expression could add prognostic value to the CAPRA-S score, which could improve the efficiency of the predicting system and lead to a more precise decision making.

Emerging evidence suggests that the immunoevasive microenvironment in PCa leads to tumor progression.<sup>18,31</sup> MDK is reported to promote tumor progression through inhibiting the recruitment of CD8<sup>+</sup> T cells in glioma and improving the polarization of M2 macrophages in melanoma.<sup>14,15</sup> Contrary to other cancer types, CD8<sup>+</sup> T cell abundance yields an unfavorable survival outcome in PCa, suggesting that CD8<sup>+</sup> T cells may display an exhausted or even immunosuppressive phenotype in PCa.<sup>16,17</sup> We thus focused on the

association between MDK expression and CD8<sup>+</sup> T cell phenotype in PCa. Indeed, tumors with high expression of MDK and high infiltration of CD8<sup>+</sup> T cells possessed the worst clinical outcome. Although the antitumor function of CD8<sup>+</sup> T cells was inhibited in tumors with MDK abundance, MDK expression was not associated with CD8<sup>+</sup> T cell infiltration in PCa. A previous study revealed that MDK impaired the antitumor function of CD8<sup>+</sup> T cells in a melanoma mice model, while the infiltration of CD8<sup>+</sup> T cells remained at the same level between melanoma with MDK overexpression and the control,<sup>14</sup> which is in accordance with our findings. We inferred that intratumoral MDK disrupted the antitumor immunity of CD8<sup>+</sup> T cells rather than acted as chemoattractant in PCa. It was previously reported that terminally exhausted CD8<sup>+</sup> T cells rather than the progenitor-exhausted CD8<sup>+</sup> T cells exhibited short lifespan and demonstrated

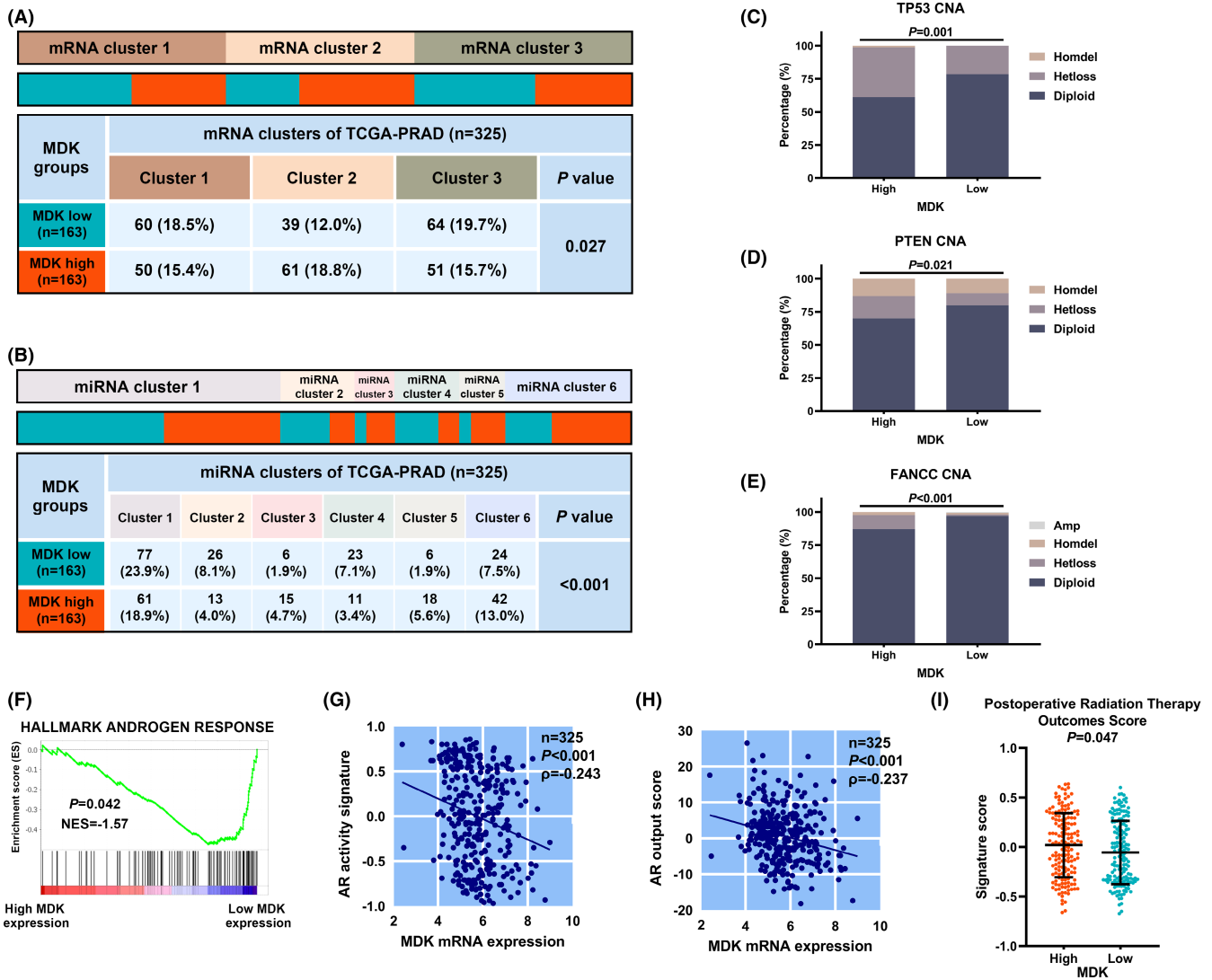


**FIGURE 5** Molecular characterization of MDK mRNA expression in PCa. (A and B) Heatmaps illustrating the distribution of mRNA clusters (A) and miRNA clusters (B) with MDK mRNA expression in external cohort ( $n = 325$ ). (C–E) Evaluation of the copy number alterations (CNA) of TP53 (C), PTEN (D) and FANCC (E) in high versus low MDK expression groups in external cohort. (F) Gene set enrichment analysis of HALLMARK ANDROGEN RESPONSE was demonstrated in high versus low MDK expression groups in external cohort. (G and H) Correlation between MDK mRNA expression and AR output score (G) or AR activity signature (H) in external cohort. (I) Evaluation of 24-gene post-Operative Radiation Therapy Outcomes Score in high versus low MDK mRNA expression groups in external cohort. Distribution of mRNA and miRNA clusters in high/low MDK mRNA expression groups were analyzed through Chi-square test. Mann-Whitney U test was applied for comparing the signature expression in high versus low MDK expression groups and  $p$  values were illustrated.

tolerance to immune checkpoint inhibition.<sup>26</sup> Enrichment of terminally exhausted T cell signature was observed in PCa with high MDK expression, which was consistent with a previous finding that MDK expression correlated with anti-PD-1/PD-L1 resistance in patients with melanoma. Importantly, our study further demonstrated that MDK modulated an immunosuppressive microenvironment with elevated expression of aggressive phenotype marker PD-L1<sup>20</sup> and increased the infiltration of M2 macrophages and tumor-promoting mast cells in PCa.<sup>27</sup> Further findings are warranted to discover the orchestration mechanism of PCa microenvironment by MDK. As MDK inhibition showed reactivated production of GZMB, PRF1, and IFN- $\gamma$  of CD8<sup>+</sup> T cells through the PDE system, we inferred

that targeting MDK in PCa may show promise. Moreover, IFN- $\gamma$  is typically reckoned as a predictor for good immunotherapy response.<sup>32,33</sup> Our study suggested a potential model that anti-MDK may sensitize PCa to anti-PD-1/PD-L1 immunotherapy, which merited exploration.

While RP still represents one of the main clinical managements, emerging studies have focused on postoperative therapies for improving patient survival.<sup>3</sup> Clinical trials for postoperative hormonal therapy including leuprorelin acetate (AFU-GETUG 20/0310) and enzalutamide (NCT01927627) are conducted for evaluating the efficacy and safety.<sup>34,35</sup> Our findings highlight the negative correlation between MDK and AR response signatures.<sup>8</sup> Moreover, a 24-gene

predictor for predicting the response to postoperative radiotherapy positively correlated with intratumoral MDK expression.<sup>10</sup> We suggested that tumors with MDK abundance may be resistant to adjuvant hormonal therapy while sensitive to postoperative radiotherapy. Whether MDK could be a predictor for postoperative adjuvant therapy deserves further investigation.

In summary, our study identified and validated intratumoral MDK expression as an independent prognosticator for postoperative clinical outcome. Tumors with MDK abundance were characterized by impaired antitumor function of tumor-infiltrating CD8<sup>+</sup> T cells, which were accompanied by enriched immunosuppressive components. Tumors with MDK enrichment were potentially sensitive to postoperative radiotherapy while resistant to adjuvant hormonal therapy of PCa. MDK could be considered as a potential therapeutic target. (Graphical abstract for the study is illustrated in Figure S10).

### FUNDING INFORMATION

This work was funded by the National Natural Science Foundation of China (No. 81872102 Haowen Jiang).

### ACKNOWLEDGMENT

This study was supported by the National Natural Science Foundation of China (81872102).

### DISCLOSURE

The authors declare no conflict of interest.

### ETHICAL APPROVAL

Approval of the research protocol by an Institutional Reviewer Board: The study was conducted after ethical approval by the Institutional Review Board of Huashan Hospital.

### INFORMED CONSENT

Signed informed consent was obtained from the participants.

### ORCID

Haowen Jiang  <https://orcid.org/0000-0002-5349-1363>

### REFERENCES

1. Rebello RJ, Oing C, Knudsen KE, et al. Prostate Cancer. *Nat Rev Dis Primers*. 2021;7:9. doi:10.1038/s41572-020-00243-0
2. Mottet N, van den Bergh RCN, Briers E, et al. EAU-EANM-ESTRO-ESUR-SIOG guidelines on prostate cancer—2020 update. Part 1: screening, diagnosis, and local treatment with curative intent. *Eur Urol*. 2021;79:243-262. doi:10.1016/j.eururo.2020.09.042
3. Tosco L, Briganti A, D'amico AV, et al. Systematic review of systemic therapies and therapeutic combinations with local treatments for high-risk localized prostate cancer. *Eur Urol*. 2019;75:44-60. doi:10.1016/j.eururo.2018.07.027
4. Cooperberg MR, Hilton JF, Carroll PR. The CAPRA-S score: a straightforward tool for improved prediction of outcomes after radical prostatectomy. *Cancer*. 2011;117:5039-5046. doi:10.1002/cncr.26169
5. D'Amico AV, Whittington R, Malkowicz SB, et al. Biochemical outcome after radical prostatectomy, external beam radiation therapy, or interstitial radiation therapy for clinically localized prostate cancer. *JAMA*. 1998;280(11):969-974. doi:10.1001/jama.280.11.969
6. Mazzone E, Gandaglia G, Ploussard G, et al. Risk stratification of patients candidate to radical prostatectomy based on clinical and multiparametric magnetic resonance imaging parameters: development and external validation of novel risk groups. *Eur Urol*. 2022;81(2):193-203. doi:10.1016/j.eururo.2021.07.027
7. Adamaki M, Zoumpourlis V. Prostate cancer biomarkers: from diagnosis to prognosis and precision-guided therapeutics. *Pharmacol Ther*. 2021;228:107932. doi:10.1016/j.pharmthera.2021.107932
8. Spratt DE, Alshalalfa M, Fishbane N, et al. Transcriptomic heterogeneity of Androgen receptor activity defines a de novo low AR-active subclass in treatment Naïve primary prostate cancer. *Clin Cancer Res*. 2019;25:6721-6730. doi:10.1158/1078-0432.CCR-19-1587
9. Zhao SG, Chang SL, Erho N, et al. Associations of luminal and basal subtyping of prostate cancer with prognosis and response to Androgen deprivation therapy. *JAMA Oncol*. 2017;3:1663-1672. doi:10.1001/jamaoncol.2017.0751
10. Zhao SG, Chang SL, Spratt DE, et al. Development and validation of a 24-gene predictor of response to postoperative radiotherapy in prostate cancer: a matched, retrospective analysis. *Lancet Oncol*. 2016;17:1612-1620. doi:10.1016/S1470-2045(16)30491-0
11. Liu D, Augello MA, Grbesa I, et al. Tumor subtype defines distinct pathways of molecular and clinical progression in primary prostate cancer. *J Clin Invest*. 2021;131(10):e147878. doi:10.1172/JCI147878
12. Abeshouse A, Ahn J, Akbani R, et al. The molecular taxonomy of primary prostate cancer. *Cell*. 2015;163:1011-1025. doi:10.1016/j.cell.2015.10.025
13. Filippou PS, Karagiannis GS, Constantinidou A. Midkine (MDK) growth factor: a key player in cancer progression and a promising therapeutic target. *Oncogene*. 2020;39:2040-2054. doi:10.1038/s41388-019-1124-8
14. Cerezo-Wallis D, Contreras-Alcalde M, Troulé K, et al. Midkine re-wires the melanoma microenvironment toward a tolerogenic and immune-resistant state. *Nat Med*. 2020;26:1865-1877. doi:10.1038/s41591-020-1073-3
15. Guo X, Pan Y, Xiong M, et al. Midkine activation of CD8<sup>+</sup> T cells establishes a neuron-immune-cancer axis responsible for low-grade glioma growth. *Nat Commun*. 2020;11:2177. doi:10.1038/s41467-020-15770-3
16. Ness N, Andersen S, Valkov A, et al. Infiltration of CD8<sup>+</sup> lymphocytes is an independent prognostic factor of biochemical failure-free survival in prostate cancer: CD8<sup>+</sup> lymphocytes in prostate cancer. *Prostate*. 2014;74:1452-1461. doi:10.1002/pros.22862
17. Leclerc BG, Charlebois R, Chouinard G, et al. CD73 expression is an independent prognostic factor in prostate cancer. *Clin Cancer Res*. 2016;22:158-166. doi:10.1158/1078-0432.CCR-15-1181
18. Zhao SG, Lehrer J, Chang SL, et al. The immune landscape of prostate cancer and nomination of PD-L2 as a potential therapeutic target. *J Natl Cancer Inst*. 2019;111:301-310. doi:10.1093/jnci/djy141
19. Zhou Q, Zhang H, Wang Z, et al. Poor clinical outcomes and immunoevasive contexture in interleukin-9 abundant muscle-invasive bladder cancer. *Int J Cancer*. 2020;147:3539-3549. doi:10.1002/ijc.33237
20. Gevensleben H, Dietrich D, Golletz C, et al. The immune checkpoint regulator PD-L1 is highly expressed in aggressive primary prostate cancer. *Clin Cancer Res*. 2016;22:1969-1977. doi:10.1158/1078-0432.CCR-15-2042
21. Kitamura H, Torigoe T, Asanuma H, Honma I, Sato N, Tsukamoto T. Down-regulation of HLA class I antigens in prostate cancer tissues and up-regulation by histone deacetylase inhibition. *J Urol*. 2007;178:692-696. doi:10.1016/j.juro.2007.03.109
22. Centenera MM, Gillis JL, Hanson AR, et al. Evidence for efficacy of new Hsp90 inhibitors revealed by ex vivo culture of human prostate tumors. *Clin Cancer Res*. 2012;18:3562-3570. doi:10.1158/1078-0432.CCR-12-0782

23. Shafi AA, Schiewer MJ, de Leeuw R, et al. Patient-derived models reveal impact of the tumor microenvironment on therapeutic response. *Eur Urol Oncol*. 2018;1:325-337. doi:10.1016/j.euo.2018.04.019
24. El-Kenawi A, Dominguez-Viqueira W, Liu M, et al. Macrophage-derived cholesterol contributes to therapeutic resistance in prostate cancer. *Cancer Res*. 2021;81:5477-5490. doi:10.1158/0008-5472.CAN-20-4028
25. Schiewer MJ, Goodwin JF, Han S, et al. Dual roles of PARP-1 promote cancer growth and progression. *Cancer Discov*. 2012;2:1134-1149. doi:10.1158/2159-8290.CD-12-0120
26. Miller BC, Sen DR, Al Abosy R, et al. Subsets of exhausted CD8+ T cells differentially mediate tumor control and respond to checkpoint blockade. *Nat Immunol*. 2019;20:326-336. doi:10.1038/s41590-019-0312-6
27. Xu W, Qian J, Zeng F, et al. Protein kinase ds promote tumor angiogenesis through mast cell recruitment and expression of angiogenic factors in prostate cancer microenvironment. *J Exp Clin Cancer Res*. 2019;38:114. doi:10.1186/s13046-019-1118-y
28. Rawnaq T, Dietrich L, Wolters-Eisfeld G, et al. The multifunctional growth factor Midkine promotes proliferation and migration in pancreatic cancer. *Mol Cancer Res*. 2014;12:670-680. doi:10.1158/1541-7786.MCR-13-0467
29. Shimwell NJ, Bryan RT, Wei W, et al. Combined proteome and transcriptome analyses for the discovery of urinary biomarkers for urothelial carcinoma. *Br J Cancer*. 2013;108:1854-1861. doi:10.1038/bjc.2013.157
30. Zhu W-W, Guo J-J, Guo L, et al. Evaluation of Midkine as a diagnostic serum biomarker in hepatocellular carcinoma. *Clin Cancer Res*. 2013;19:3944-3954. doi:10.1158/1078-0432.CCR-12-3363
31. Wu Z, Chen H, Luo W, et al. The landscape of immune cells infiltrating in prostate cancer. *Front Oncol*. 2020;10:517637. doi:10.3389/fonc.2020.517637
32. Liu D, Schilling B, Liu D, et al. Integrative molecular and clinical modeling of clinical outcomes to PD1 blockade in patients with metastatic melanoma. *Nat Med*. 2019;25:1916-1927. doi:10.1038/s41591-019-0654-5
33. Gide TN, Quek C, Menzies AM, et al. Distinct immune cell populations define response to anti-PD-1 monotherapy and anti-PD-1/anti-CTLA-4 combined therapy. *Cancer Cell*. 2019;35:238-255.e6. doi:10.1016/j.ccell.2019.01.003
34. Rozet F, Habibian M, Berille J, et al. A phase III randomized, open-label multicenter trial to evaluate the benefit of leuprorelin acetate for 24 months after radical prostatectomy in patients with high risk of recurrence (AFU-GETUG 20/0310). *JCO*. 2012;30:252. doi:10.1200/jco.2012.30.5\_suppl.252
35. Ornstein MC, Stephenson AJ, Elson P, et al. Adjuvant enzalutamide (Enza) for men with non-metastatic high-risk prostate cancer (HRPCa) after radical prostatectomy (RP). *JCO*. 2018;36:88. doi:10.1200/JCO.2018.36.6\_suppl.88

## SUPPORTING INFORMATION

Additional supporting information can be found online in the Supporting Information section at the end of this article.

**How to cite this article:** Zhou Q, Yang C, Mou Z, et al. Identification and validation of a poor clinical outcome subtype of primary prostate cancer with Midkine abundance. *Cancer Sci*. 2022;113:3698-3709. doi: [10.1111/cas.15546](https://doi.org/10.1111/cas.15546)